Contemporary Engineering Sciences, Vol. 11, 2018, no. 98, 4879 - 4890
HIKARI Ltd, www.m-hikari.com
https://doi.org/10.12988/ces.2018.88471

Neurofuzzy Modelling of Lung Sounds

George Kandilogiannakis and Paris Mastorocostas

Department of Informatics & Computer Engineering
University of West Attica
12244, Egaleo, Greece

Dimitris Varsamis and Costas Hilas

Department of Informatics Engineering
Technological Educational Institute of Central Macedonia - Serres
62124, Serres, Greece

Abstract

In this paper a computational intelligence-based filter for real-time separation the adventitious discontinuous lung sounds from the vesicular sounds is proposed. The filter uses two Dynamic Fuzzy Neural Networks to perform the task of separation of the lung sounds, obtained from patients with pulmonary pathology. The networks are trained by the Simulated Annealing Dynamic Resilient Propagation algorithm and the resulting filter is applied to three major classes of lung sounds. In order to highlight the learning characteristics and the performance of the proposed separation scheme, extensive experimental analysis is conducted, where a comparison with other filters is given.

Keywords: lung sounds, fuzzy neural network, internal feedback, simulated annealing

1 Introduction

Nowadays, the field of bioinformatics has gained a lot of research interest, with two of the most active hottest topics being the study of biomedical signals and

the development of processing tools [1]. The analysis of lung sounds constitute an important issue in the area, and a series of identification and separation techniques regarding lung sounds have been proposed [2]-[3]. Pathological discontinuous adventitious sounds (DAS) are strongly related to pulmonary dysfunction, therefore their efficient identification and separation form the normal vesicular sounds (VS) can contribute to the interpretation of respiratory malfunction. Among the processing methods that have been introduced in the past, the wavelet transform-based stationary-nonstationary (WTST-NST) filter [4] has been proved to provide the most accurate separation results. However, this method cannot be easily implemented in real-time analysis of lung sounds. In order to alleviate this issue, various neural and fuzzy models have been proposed during the last two decades. In [5] and [6], fuzzy modelling has been employed for performing real-time separation of DAS (nonstationary waves) from VS (stationary waves). These filters consist of two fuzzy inference systems that operate in parallel and their outputs are the nonstationary and the stationary signals.

Even though the aforementioned filters perform real-time separation quite effectively, they are static models, attempting to capture the plant dynamics by feeding the networks with delayed values of the input signal. In order to address more efficiently the nature of these signals, recurrent neural [7] and neurofuzzy models [8]-[9] have been proposed. These dynamic systems provided improved separation performance.

Stem from the above fact, in the present work the recurrent filter introduced in [9] is combined with an efficient learning algorithm, the Simulated Annealing Dynamic Resilient Propagation ([10]), which constitutes a blending of an enhanced gradient-based learning method with Simulated Annealing. The filter consists of two neurofuzzy systems, for the estimation of both the stationary and the stationary part of lung sounds.

The paper is organized as follows: Section 2 hosts a brief description of the Dynamic Fuzzy Neural Network. In section 3 the structure characteristics of the learning algorithm are illustrated. The filters structure is presented in Section 4, followed by extensive experimental results, regarding the three major classes of lung sounds. The concluding remarks are given in Section 5.

2 The Dynamic Fuzzy Neural Network

The neurofuzzy model employed in this work is the Dynamic Fuzzy Neural Network (DFNN), introduced in [11]. The main feature of this fuzzy model is that the consequent parts of its fuzzy rules are recurrent neural networks:

$$\begin{aligned} &R^{(l)} : IF u_1(k) \text{is} A_1^l ... AND u_m(k) \text{is} A_m^l \\ &THEN \hat{y}_l(k) = RNN_l\left(u(k)\right) = RNN_l(u(k)) \end{aligned} \tag{1}$$

where RNN_l is a recurrent neural network for the consequent part of the l-th rule, of the form $mH1$, with m and H being the numbers of neurons in the input and hidden layers, respectively. The output layer comprises a single neuron, that provides the rule output $\hat{y}(k)$.
The output of the model at time k is determined using the weighted average defuzzification method:

$$\hat{y}(k) = \frac{\sum_{l=1}^{r} \mu_l(k) \cdot \hat{y}_l(k)}{\sum_{l=1}^{r} \mu_l(k)} \tag{2}$$

The degree of fulfilment of the l-th rule is given by

$$\mu_l(k) = \prod_{i=1}^{m} \mu_{A_i^l}(u_i(k)) \tag{3}$$

where $\mu_{A_i^l}(u_i)$ are Gaussian membership functions, with m_i^l and σ_i^l being the mean value and standard deviation, respectively, of the fuzzy set that corresponds to the i-th input variable. The operation of RNN_l is described by the following set of equations:

$$O_{li}^1(k) = f_1\left(\sum_{j=1}^{m}\sum_{q=0}^{O_u} w_{ijq}^{1(l)} \cdot u_j(k-q) + \sum_{j=1}^{Oy_1} w_{ij}^{2(l)} \cdot O_{li}^1(k-j) + w_i^{3(l)}\right) \tag{4}$$

$$\hat{y}_l(k) = f_2\left(\sum_{i=1}^{H}\sum_{q=0}^{Oy_3} w_{iq}^{4(l)} \cdot O_{li}^1(k-q) + \sum_{j=1}^{Oy_2} w_j^{5(l)} \cdot \hat{y}_l(k-j) + w^{6(l)}\right) \tag{5}$$

where the following notation is used:

- f_1, f_2 are the neuron activation functions (hyperbolic tangent) of the hidden and the output layers, respectively.
- O_u is the time lag order of the input signal. Accordingly, O_u and O_{y_1} refer to the inputs and the local output feedback, respectively, for the hidden layer neurons, while O_{y_3} and O_{y_2} refer to the inputs and the local output feedback, respectively, for the output neuron.
- $O_{li}^1(k)$ is the output of the i-th hidden neuron at time k.
- $w_{ijq}^{1(l)}$ and $w_{ij}^{2(l)}$ are FIR and IIR synaptic weights at the hidden layer, $w_{jq}^{4(l)}$ and $w_j^{5(l)}$ are FIR and IIR synaptic weights at the output layer, and $w_i^{3(l)}$ and $w^{6(l)}$ are bias terms for the hidden neurons and the output neuron, respectively.

Since the DFNN comprises fuzzily interconnected recurrent sub-systems, its architecture preserves the local modelling approach of classic fuzzy models. The rules are not linked with each other in time, neither through external nor internal feedback; they are connected merely via the defuzzification part. Moreover, since the system is a single-input one, the complexity of the premise part is kept to a minimum and the rule base does not suffer from the curse of dimensionality. Additionally, the use of neurons with internal feedback leads to a network with rich internal recurrence, thus increasing the representation capabilities of the network and permitting the identification of complex temporal dependencies.

3 The Learning Algorithm

The Simulated Annealing Dynamic Resilient Propagation (SA-DRPROP), presented in [10] for the case of DFNN, ameliorates the learning abilities of the standard gradient-based learning methods, by alleviating the problem of trapping to local minima and by expanding the search in the weight space. In brief, let $\frac{\partial^+ E(t)}{\partial w_i}$ and $\frac{\partial^+ E(t-1)}{\partial w_i}$ denote the derivatives of an error function E with respect to a models weight w_i at the present and the preceding epochs, respectively. In SA-DRPROP each fitting parameter has its individual step size, which is adjusted during the learning process based on the sign of the respective partial derivative at the current and the previous epoch. Therefore, the effect of the adaptation process is not blurred by the influence of the size of the parameter gradient but is only dependent on the temporal behavior of the gradient. SA-DRPROP is described in pseudo-code as follows:

(a) For all weights w_i initialize the step sizes $\Delta_i^{(1)} = \Delta_0$, Repeat

(b) For all weights w_i compute the SA-DRPROP error gradient:

$$\frac{\partial^+ E(t)}{\partial w_i} - 0.01 \cdot SA \cdot \frac{w_i}{1 + w_i^2}$$

(c) For all weights w_i, update step sizes:

(c.1) If $\frac{\partial^+ E(t)}{\partial w_i} \times \frac{\partial^+ E(t-1)}{\partial w_i} > 0$
Then $\Delta_i^{(t)} = \min \left\{ \eta^+ \cdot \Delta_i^{(t-1)}, \Delta_{\max} \right\}$

(c.2) Else if $\frac{\partial^+ E(t)}{\partial w_i} \times \frac{\partial^+ E(t-1)}{\partial w_i} < 0$
Then If $\left(\Delta_i^{(t)} < 0.4 \cdot SA^2 \right)$
Then $\Delta_i^{(t)} = \max \left\{ \eta^- \cdot \Delta_i^{(t-1)} \cdot 0.8 \cdot r \cdot SA^2, \Delta_{\min} \right\}$
Else $\Delta_i^{(t)} = \max \left\{ \eta^- \cdot \Delta_i^{(t-1)}, \Delta_{\min} \right\}$

(c.3) Else $\Delta_i^{(t)} = \Delta_i^{(t-1)}$

(d) Update weights w_i : $\Delta w_i(t) = -sign\left(\frac{\partial^+ E(t)}{\partial w_i}\right) \cdot \Delta_i^{(t)}$, Until convergence

where the step sizes are bounded by Δ_{min}, Δ_{max}. The increase and attenuation factors are usually set $n^+ \in [1.1, 1.3]$ and $n^- \in [0.5, 0.8]$, respectively. The term $SA = 2^{-r \cdot Temp}$ is the *simulated annealing term*, parameter r takes random values within the interval $[0, 1]$ and $Temp$ is the temperature.
The step (c.2) aims at adding noise to the weights, according to the concept of simulated annealing, in order to increase the convergence speed of the learning process. In SA-DRPROP, noise is added to the weight update values when the error gradient changes sign in two successive epochs, and the magnitude of the update value is less than a value that is proportional to the SA term. In this way, the weight update is modified by noise only when it has a relatively small value, thus allowing the weight to move out of local minima, while minimizing the disturbance to the adaptation process.
Additionally, in (b) a weight decay term is added to the error gradient, as proposed in [12], in order to modify the error surface such that initially weights with lower values are favored. As training proceeds, the magnitude of weight decay is reduced, facilitating the increase of bigger weights and allowing the model to explore regions of the error surface that were previously unavailable. As far as the extraction of the error gradients is concerned, it is fully described in [10].

4 Experimental Results

The filter consists of two DFNN networks that operate in parallel, for estimating the non-stationary (DAS) and the stationary (VS) parts of the input signal. The input signal $u(k)$ is the normalized zero-mean recorded lung sound. Therefore, the outputs of the filter are estimations of the DAS (y_{NST}) and the VS (y_{ST}).
The training data sets comprise ten cases per signal category, drawn from the lung sound databases [13]-[15], where they have been filtered in order to avoid aliasing. The lung sounds are divided into three categories: (a) the fine crackles (FC), taken from patients with pulmonary and interstitial fibrosis, (b) the coarse crackles (CC), corresponding to patients with chronic bronchitis, and (c) the squawks (SQ), which are related to patients with interstitial fibrosis and allergic alveolitis.
The data sets have been obtained by digitizing sections of 15sec of the filtered signals by a 12-Bit Analog-to-Digital (A/D) converter at a sampling rate of 2.5kHz, divided into successive records of 1024 or 2048 samples each, with zero mean value and normalized. Then, all these records have been processed by

the WTST-NST filter, [4], in order to obtain an accurate estimation of their stationary and non-stationary parts. Therefore, the stationary and nonstationary outputs of the WTST-NST filter are considered to be the desired ones. Training is conducted independently for each network and signal category, leading to three filters and six networks. Extensive trials have been carried out in order to determine the optimal structural characteristics of the networks, which are given in Table 1 Training lasts for 1000 epochs and the learning parameters, common to all six models, are also presented in Table 1.

Table 1: Structural and learning parameters

Model	Rules	Ou	Oy_1	Oy_2	Oy_3	H	Learning parameters
FCst	2	2	2	4	4	2	Temp 1.2
FCnst	7	2	2	4	4	3	1.05
CCst	5	2	2	2	2	3	0.5
CCnst	4	1	2	2	1	4	1E-4
SQst	4	1	2	2	1	4	1E-2
SQnst	5	2	2	4	4	3	

The results obtained using the proposed filter are evaluated by the following measures:

- Auditory inspection of the filters stationary output, by listening to its stationary outputs after digital-to-analog (D/A) conversion.
- The rate of detectability: $D_R = \left(1 - \frac{N_R - N_E}{N_R}\right) \cdot 100\%$, where N^E is the number of estimated DAS and N^R is the number of visually recognized DAS by a physician (considered as the true number of DAS in the input signal).
- The root mean squared error: $RMSE = \frac{1}{k_f} \sum_{k=1}^{k_f} \left[y(k) - \hat{y}(k)\right]^2$, where $y(k)$ is the filters output (stationary or nonstationary) of the k-th sample, $\hat{y}(k)$ is the respective actual output and k_f is the number of samples.

It should be noted that the values of the RMSE do not always represent good separation results; they do not focus on the particular signal details a physician is interested in. They are only intended to provide an indication of the degree to which the desired input-output relation has been identified, given the evaluation by the first two criteria. The results of the evaluation according

to the aforementioned criteria are hosted in Table 2.
It becomes clear that the proposed filter is capable of separating DAS from VS quite effectively, since the rate of detectability is 100% in 13 out of 16 cases and very high in the rest 3 cases. In addition, the qualitative testing of the filter which was conducted by listening to its stationary outputs after Digital-to-Analog conversion, was almost perfect, since the DAS were practically not heard.
It should be mentioned that in all three filters the required calculations of the DFNN networks (multiplications, additions and look-up table operations) are rather limited. In particular, the maximum number of multiplications (the most time-consuming kind of operation) is 154, which can be delivered by a standard PC or dedicated modern hardware within the sampling period (0.4ms). Thus, real-time operation is accomplished, which constitutes a key factor for efficient clinical screening of DAS.

In order to have a visual representation of the filters performance, recorded pathological lung sounds, separated coarse crackles and vesicular sounds are depicted in parts (a), (b) and (c) of Figure 1, respectively, representing case C7, which was recorded from two patients with chronic bronchitis. The position of waves identified visually by a physician as crackles were marked with arrowheads. It becomes evident from Figure 1(b) that all DAS sounds shown in Figure 1(a) are easily identified, since their morphologies and locations are clearly distinguished. From Figure 1(c) it can be noted that the stationary outputs are almost identical to the pure vesicular sounds.
In Figure 2(a) the case C16 of squawks is displayed. Despite their large concentration, their characteristics are clearly identified in the non-stationary output, as shown in Figure 2(b). The vesicular sound is accurately reconstructed in the stationary output, as depicted in Figure 2(c).

Figure 3 displays a significant advantage of the SA-DRPROP algorithm; its robustness to initial conditions. The z-score transform of the RMSE for the nonstationary and stationary outputs for the FC filter is hosted in Figure 3(a)-(b), for a series of 35 trials with different initial conditions. It can be seen that the resulting values of the transform lie within the relatively narrow intervals [-3, 1] and [-1.5, 2]. Similar results are attained for the classes of coarse crackles and squawks.

A comparative analysis is conducted in the sequel, with the competing rivals of the proposed filter being WTST-NST [4], the fuzzy filters FST-NST [5] and OLS-FF [6], as well as the recurrent neural network BDRNN [7]. All filters are applied to the same cases of patients and the results are shown in Table 3.

According to the aforementioned results, becomes obvious that the proposed filter exhibits a significantly improved separation performance and a reduced RMSE compared to the static filters, due to the recurrent models

Table 2: Filters performance

Case	DAS	Diagnosis	N	NE/NR	$DR(\%)$	$RMSE_{ST}$	$RMSE_{NST}$
C1	FC	PF	2048	18/18	100	0.04244	0.03821
C2	FC	PF	1024	7/7	100	0.04720	0.04661
C3	FC	PF	1024	8/9	88.88	0.05515	0.05242
C4	FC	PF	1024	9/9	100	0.03595	0.03901
C5	FC	PF	1024	10/11	90.90	0.04451	0.04327
C6	FC	IF	2048	19/19	100	0.06330	0.06018
C7	CC	CB	2048	7/7	100	0.04519	0.04382
C8	CC	CB	2048	7/7	100	0.05246	0.05276
C9	CC	CB	1024	8/8	100	0.07478	0.06211
C10	CC	CB	1024	8/8	100	0.08390	0.09600
C11	CC	CB	1024	10/11	90.90	0.06913	0.08147
C12	SQ	IF	1024	2/2	100	0.05638	0.05492
C13	SQ	IF	1024	4/4	100	0.06348	0.06199
C14	SQ	IF	1024	5/5	100	0.08397	0.08142
C15	SQ	AA	1024	6/6	100	0.06037	0.06569
C16	SQ	AA	2048	26/26	100	0.05236	0.05103

- PF: Pulmonary Fibrosis; IF: Interstitial Fibrosis
- CB: Chronic Bronchitis; AA: Allergic Alveolitis
- N: Number of samples
- RMSEST / RMSENST: RMSE of the estimated stationary/nonstationay output of the filter

ability to track the dynamics of the nonstationary signal. Compared to the other recurrent model, the proposed filter provides similar results with respect to the RMSE, but has an improved average rate of detectability for the case of fine crackles.

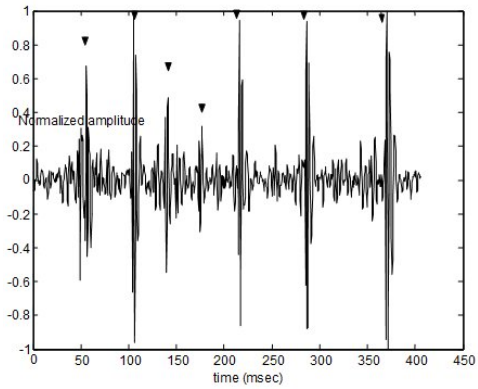

(a)

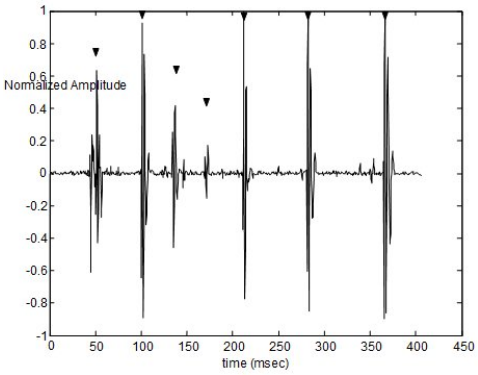

(b) DAS

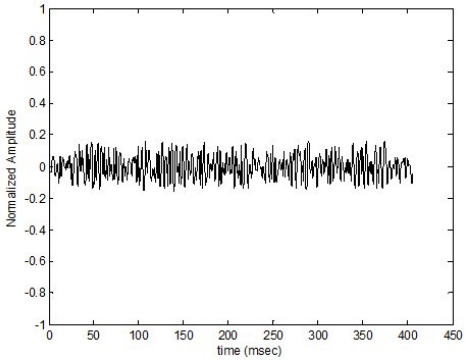

(c) VS

Figure 1: A case of coarse crackles

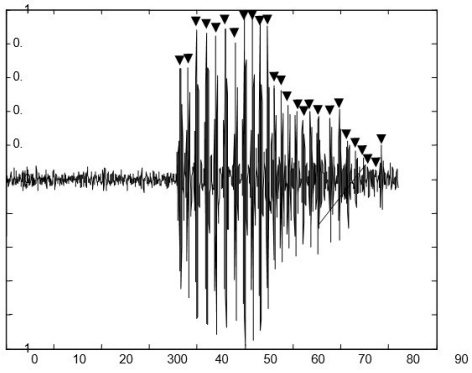

(a)

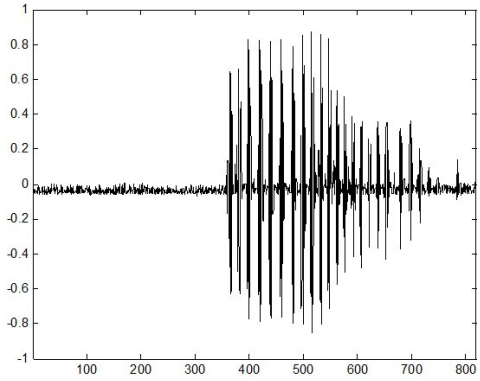

(b) DAS

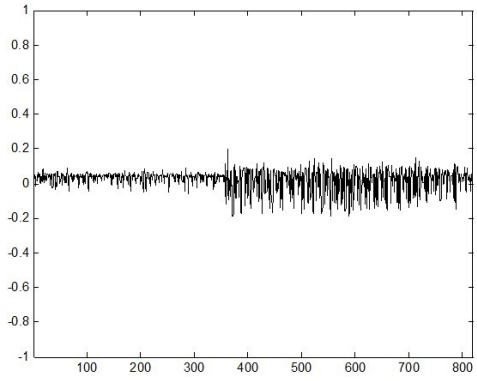

(c) VS

Figure 2: A case of squawks

5 Conclusion

A neurofuzzy filter for separating lung sounds has been proposed. It consists of two fuzzy neural networks with internal feedback and is trained by a hybrid algorithm, which combines a gradient-based method with simulated annealing. The filter has been tested on the classes of fine crackles, coarse crackles and

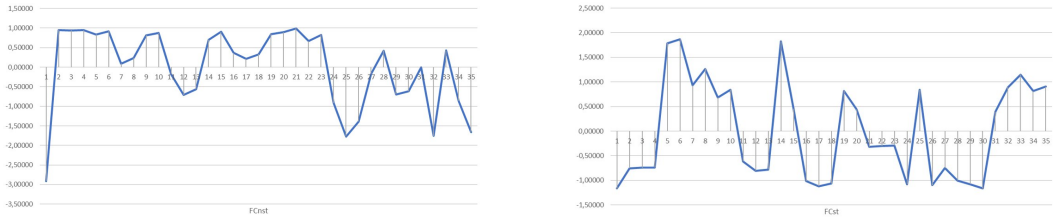

(a) Nonstationary output (b) Stationary output

Figure 3: z-score transform for the class of Fine Crackles

Table 3: Performance evaluation with other filters

Fine Crackles	WTST-NST	FST-NST	OLS-FF	BDRNN	Proposed
$\bar{TD}_R$	100	92.82	80.50	93.90	96.63
RMSEst	ND	0.0485	0.0488	0.0474	0.0482
RMSEnst	ND	0.0621	0.0484	0.0494	0.0466
Coarse Crackles	WTST-NST	FST-NST	OLS-FF	BDRNN	Proposed
$\bar{TD}_R$	97.5	95.68	96.36	98.18	98.18
RMSEst	ND	0.0632	0.0679	0.0647	0.0650
RMSEnst	ND	0.0749	0.0711	0.0638	0.0672
Squawks	WTST-NST	FST-NST	OLS-FF	BDRNN	Proposed
$\bar{TD}_R$	100	94.46	96.36	100	100
RMSEst	ND	0.0711	0.0679	0.0633	0.0633
RMSEnst	ND	0.0761	0.0664	0.0650	0.0630

ND: Not Defined

squawks, exhibiting a very efficient separation performance. Moreover, due to the limited number of arithmetic operations, the proposed filter is capable of conducting real-time separation, thus improving the procedure of clinical screening of lung sounds.

Acknowledgements. This work was supported in part by the Postgraduate Program in Applied Information Systems of Piraeus University of Applied Sciences.

References

[1] A. Badnjevic, L. Gubeta and E. Custovic, An Expert Diagnostic System to Automatically Identify Asthma and Chronic Obstructive Pulmonary Disease in Clinical Settings, *Scientific Reports,* **8** (2018), 1–9. https://doi.org/10.1038/s41598-018-30116-2

[2] X. Lu and M. Bahoura, An Integrated Automated System for Crackles Extraction and Classification, *Biomedical Signal Processing and Control,* **3** (2008), 244–254. https://doi.org/10.1016/j.bspc.2008.04.003

[3] D. Bardou, K. Zhang and S. Ahmad, Lung Sounds Classification Using Convolutional Neural Networks, *Artificial Intelligence in Medicine,* **88** (2018), 58–69. https://doi.org/10.1016/j.artmed.2018.04.008

[4] L. Hadjileontiadis and S. Panas, Separation of Discontinuous Adventitious Sounds from Vesicular Sounds Using a Wavelet-Based Filter, *IEEE Transactions on Biomedical Engineering,* **44** (1997), 1269–1281. https://doi.org/10.1109/10.649999

[5] Y. Tolias, L. Hadjileontiadis and S. Panas, Real-Time Separation of Discontinuous Adventitious Sounds from Vesicular Sounds Using a Fuzzy Rule-based Filter, *IEEE Transactions on Information Technology in Biomedicine,* **2** (1998), 204–215. https://doi.org/10.1109/4233.735786

[6] P. Mastorocostas, Y. Tolias, J. Theocharis, L. Hadjileontiadis and S. Panas, An Orthogonal Least Squares-Based Fuzzy Filter for Real-Time nalysis of Lung Sounds, *IEEE Transactions on Biomedical Engineering,* **47** (2007), 1165–1176. https://doi.org/10.1109/10.867921

[7] P. Mastorocostas and J. Theocharis, A Stable Learning Method for Block-Diagonal Recurrent Neural Networks: Application to the Analysis of Lung Sounds, *IEEE Transactions on Systems, Man, and Cybernetics, Part B: Cybernetics,* **36** (2006), 242–254. https://doi.org/10.1109/tsmcb.2005.856722

[8] M. Khodabakhshi and M. Moradi, The Attractor Recurrent Neural Network Based on Fuzzy Functions: An Effective Model for the Classification of Lung Abnormalities, *Computers in Biology and Medicine,* **84** (2017), 124–136. https://doi.org/10.1016/j.compbiomed.2017.03.019

[9] P. Mastorocostas and J. Theocharis, A Dynamic Fuzzy-Neural Filter for Separation of Discontinuous Adventitious Sounds from Vesicular Sounds, *Computers in Biology and Medicine,* **37** (2007), 60–69. https://doi.org/10.1016/j.compbiomed.2005.10.006

[10] P. Mastorocostas and . Rekanos, Simulated annealing Dynamic RPROP for Training Recurrent Fuzzy Systems, *Proceeding of the 14th IEEE International Conference on Fuzzy Systems, Reno, U.S.A.,* (2005), 1086–1091. https://doi.org/10.1109/fuzzy.2005.1452546

[11] P. Mastorocostas and J. Theocharis, A Recurrent Fuzzy Neural Model for Dynamic System Identification, *IEEE Transactions on Systems, Man, and Cybernetics, Part B: Cybernetics,* **32** (2002), 176–190. https://doi.org/10.1109/3477.990874

[12] N. Treadgold and T. Gedeon, Simulated Annealing and Weight Decay in Adaptive Learning: The SARPROP Algorithm, *IEEE Transactions on Neural Networks,* **9** (1998), 662–668. https://doi.org/10.1109/72.701179

[13] S. Kraman, *Lung Sounds: An Introduction to the Interpretation of the Auscultatory Finding*, Northbrook, IL: Amer. College of Chest Physicians, 1993, audio tape.

[14] S. Lehrer, *Understanding Lung Sounds*, Philadelphia, PA: Saunders, 1993, audio tape.

[15] A. Tilikian, *Understanding Heart Sounds and Murmurs with an Introduction to Lung Sounds*, Philadelphia, PA: Saunders, 1993, audio tape.

Received: September 10, 2018; Published: November 22, 2018